2016

An examination of the CMB large-angle suppression

Ellis Herman
University of Richmond

An Examination of the CMB Large-Angle Suppression

By

Ellis Herman

Honors Thesis

Submitted to

Department of Physics

University of Richmond

Richmond, VA

Advised by Dr. Ted Bunn and Dr. Arthur Kosowsky

March 23, 2016

Table of Contents

Abstract

As shown by COBE-DMR and then by the Wilkinson Anisotropy Probe (WMAP), there exists an anomaly in the correlation function of the cosmic microwave background (CMB) radiation, namely that said correlation function is suppressed to zero on large angular scales. This observation conflicts with the prediction made by Lambda-CDM, the standard model of cosmology, indicating either necessary changes to the standard model or that our universe is a rare fluke within LCDM - such suppressions are seen in only about 0.3% of universes predicted by LCDM. To differentiate into which of these categories our universe falls, we have attempted to use a suppressed correlation function to generate a power spectrum. Once we are successful in generating this power spectrum, we will use the Cosmic Linear Anisotropy Solving System, or CLASS, to predict polarization and large-scale structure maps.

Scientific Background

Cosmic Microwave Background Radiation (CMB)

The cosmic microwave background radiation is a field of microwave radiation present throughout the universe at a near constant temperature of 2.72548 K, which varies by 0.00057 K. These variations in temperature can be seen in Figure 1 below, where red represents higher than average temperatures and blue represents cooler than average temperatures.

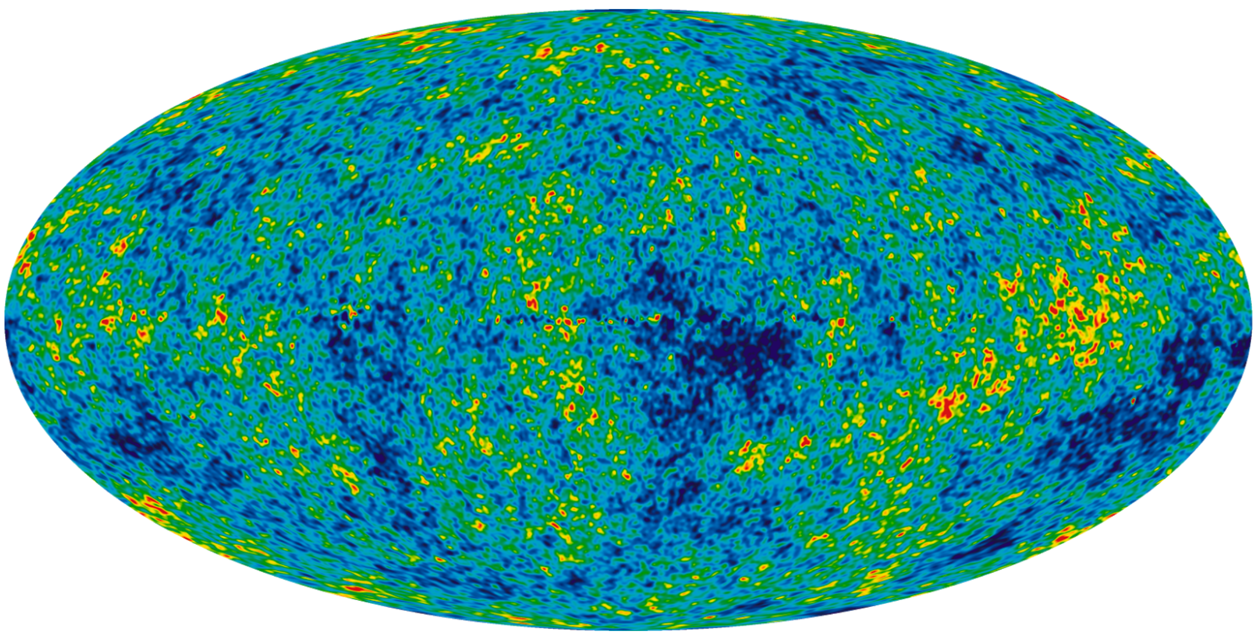

Figure 1: Full-sky image derived from nine years' WMAP data. NASA (2012)

The CMB is thermal radiation left over from the time of recombination, about 400,000 years after the Big Bang. This time scale is shown in Figure 2, below. During recombination, the universe cooled to the point that many protons and electrons joined to become neutrons and the mean free path of photons grew immensely. The long distances photons could then travel caused the universe to go from opaque to transparent. This transparency released the radiation that is only now reaching the Earth, which we call the CMB.

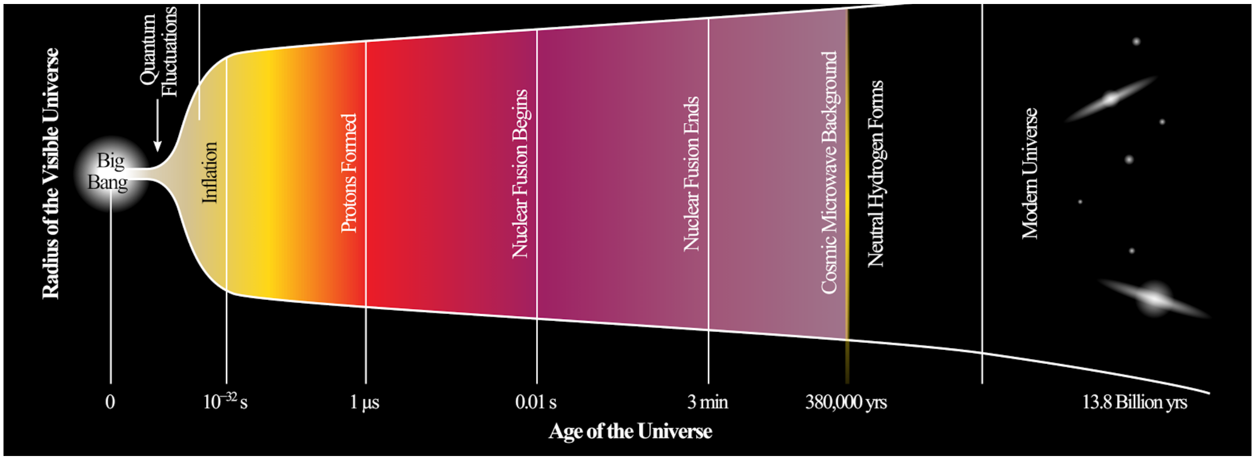

Figure 2: Time scales of the universe. National Science Foundation (2014)

As the universe was opaque until the time of recombination no light was released before the CMB, making it the oldest light in the universe. This age makes CMB cosmologists' best evidence to learn about the early universe and thus the largest scales in the present universe. It provided crucial evidence for the Big Bang theory, as well as the inspiration for the theory of inflation. Thus, the CMB informs cosmologists of the state of the universe from its very beginnings until, by use of the power spectrum, the large-scale structures of the present day.

In any raw map of the CMB, the Milky Way clouds the center of the map, seen in Figure 3, below. Because cosmologists' interest lies outside of this galaxy, the Milky Way's presence in the map posed a problem. In order to remove it, images are taken at varying frequencies. Because the variations in frequency of the radiation in our own galaxy are known, we are then able to create a full-sky map showing only the CMB. These images taken at different frequencies are shown in Figure 4, below.

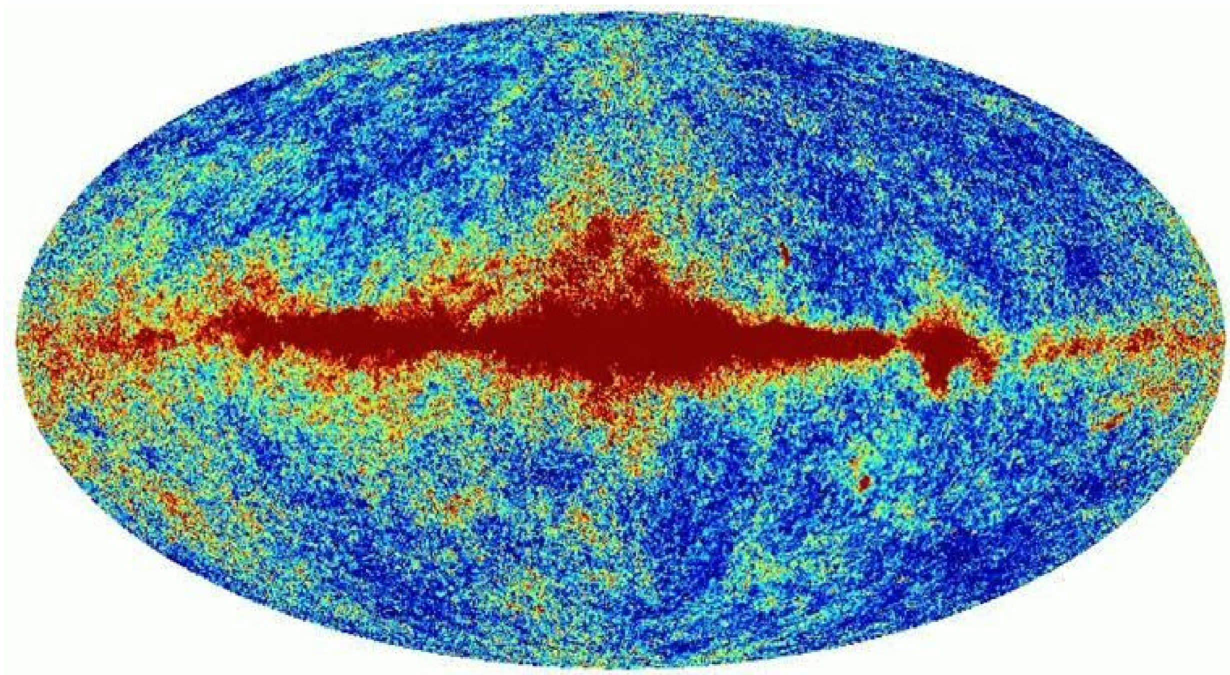

Figure 3: Full-sky map with Milky Way foreground contamination. WOMBAT (1999)

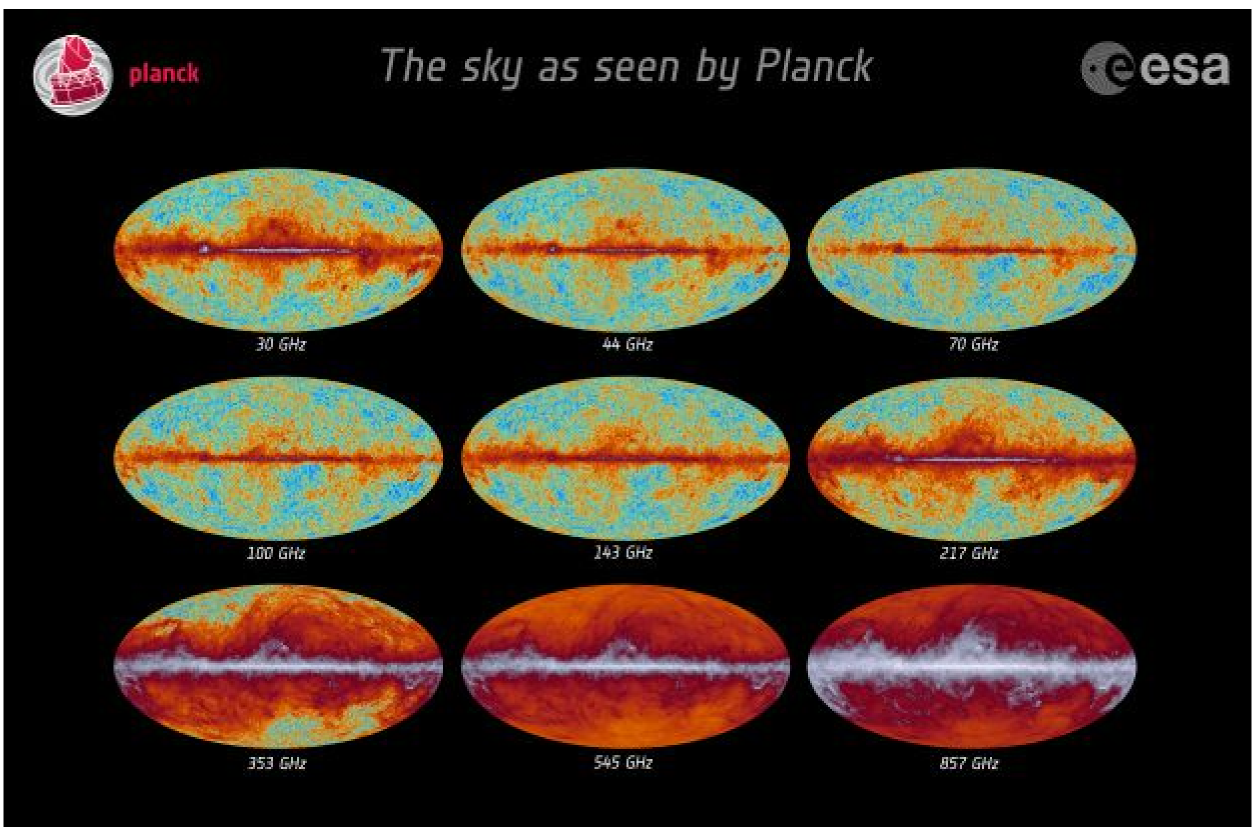

Figure 4: Removal of the Milky Way from the full-sky map. ESA (2013)

Power Spectrum

The power spectrum is denoted P(k), where k is wavenumber (or 1/wavelength) and is a Fourier transform of the three-dimensional density function. Density gives rise to temperature, as well as polarization and large scale structures. A graph of the power spectrum is shown below, in Figure 5.

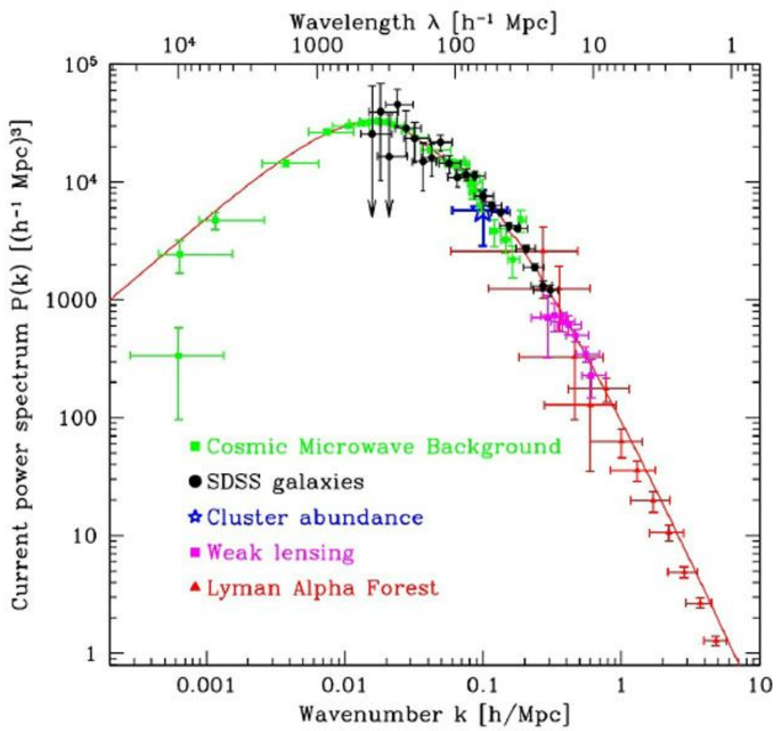

Figure 5: Power Spectrum as a function of wavenumber. Tegmark, M. et al (2004)

Figure 5 includes measurements of the CMB, SDSS galaxies, cluster abundance, and Lyman Alpha Forest (these three indicate large-scale structure) and weak lensing. The standard model of cosmology's power spectrum is displayed as the red line. In general, the observations agree with the theory; at low wavenumbers, however, the CMB no longer fits the standard model's prediction. This discrepancy corresponds to the anomaly seen in the correlation function, discussed further below.

Correlation Function

The two-point correlation function measures the average correlation between all points in the full-sky separated by theta. The correlation function is generally denoted

$$C(\theta) = \langle \delta T(n)\, \delta T(n') \rangle \quad (1$$

where theta is the angle of separation, n is a point on the map, n' is a point separated from n by theta degrees, and δT(n) and δT(n') are the deviations of the temperatures of n and n' from the mean temperature. These temperatures are then averaged over every point separated from n by theta degrees, and then over every point in the map. This process results in the correlation function's value for that theta. It is important to note that the correlation function in this paper uses distance rather than angle. Despite using a different metric, the concept is the same. This explanation is given using an angular correlation function because it is somewhat easier to see. As can be observed from Equation 1, if both points are cooler than average or if both are warmer than average, the correlation would be positive. If one is warmer than average and one is cooler than average, however, the correlation would be negative. Figure 6, below, shows an illustration of the correlation function.

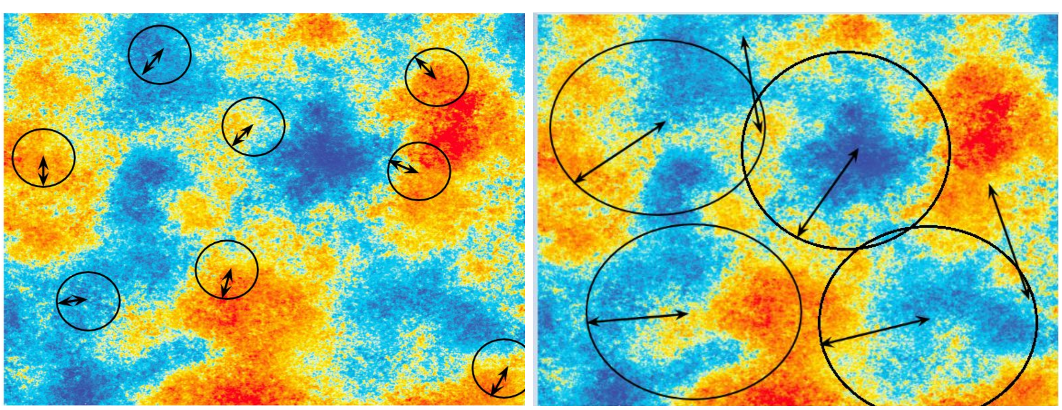

Figure 6: Illustration of the correlation function. Chiacchia, Ken (2012)

The image on the left shows the correlation function taken at small angular scales; since the angle is small, most of the points on the circles (the points separated from the middle by theta) deviate from the mean temperature similarly to the middle point - if the middle is warmer than average, most of the points separated from it by theta also are. The image on the right, however, shows the correlation function at larger angular scales. In this image, it is not clear whether points along the circles share the deviation from the mean temperature of the central point. The full correlation function, from 0 to 180 degrees is shown below, displaying several observed maps, as well as the correlation function predicted by the standard model of cosmology.

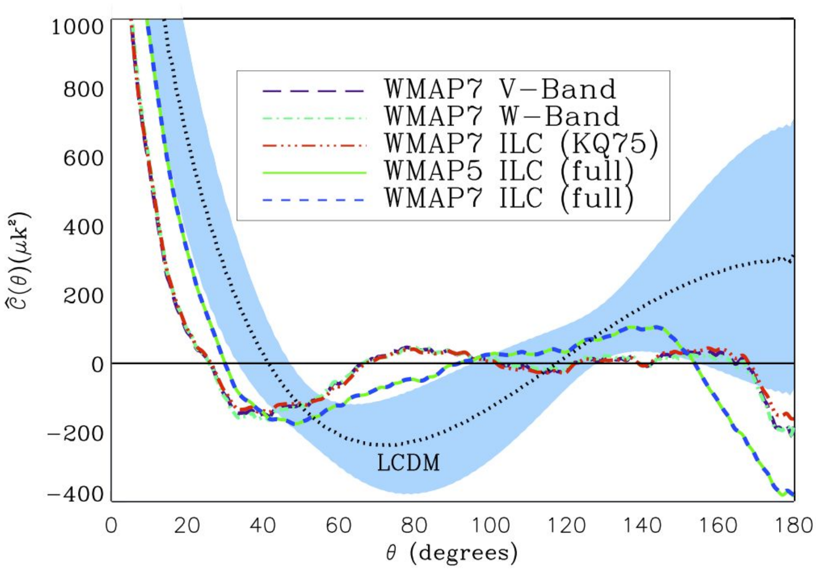

Figure 6: LCDM Two-Point Correlation Function. Sarkar et al. (2010)

Large-Angle Suppression

Figure 6, above, shows the problem this paper investigates. While the observed correlation function matches the standard model's (LCDM) prediction at low-angles, at large-angles there is a noticeable difference; the theory predicts a positive correlation above 120 degrees, but the observed correlation function goes to zero above 60 degrees. This "large-angle suppression" has been explored by a group including Craig J. Copi of Case Western Reserve University, Dragan Huterer of the University of Michigan, Dominik J. Schwarz of the University of Bielefeld,and Glenn D. Starkman of CERN in *Large-Angle CMB Suppression and Polarization Predictions*. In this paper, the authors discuss their development of a statistic with a 25 percent chance of determining that this suppression is not a "fluke" with 99.9 percent confidence.[1] Unfortunately, because the signal-to-noise ratio in the polarization data is not yet sufficient, this group's work only describes a prescription, without the results of the procedure.

Methods

As stated above, this paper explores the large-angle suppression seen in the correlation function of the CMB temperature map. This suppression is seen in only 0.3% of universes predicted by the standard model of cosmology. To examine whether this suppression indicates a flaw in the standard model or whether it is indeed a anomaly, we have introduced a suppression into the LCDM correlation function to mimic what is observed (and shown by the WMAP data displayed in Figure 6). Then, using a Fourier transform, we found the power spectrum resulting from the suppressed correlation function. Finally, using CLASS (Cosmic Linear Anistropy Solving System), we used this power spectrum to generate large-structure and polarization maps.

This work was started at the University of Pittsburgh under the supervision of Dr. Arthur Kosowsky and graduate student Simone Aiola during the summer of 2015,

---

[1] http://arxiv.org/pdf/1303.4786v2.pdf

before being continued at the University of Richmond under the supervision of Dr. Ted Bunn during the fall of 2015 and spring of 2016. In both locations, the work involved the using of writing programs using the computer language python, as well as the python package healpy, used to manipulate healpix maps and based on visualization tools used in python.

Our eventual goal was to write a program that could generate a power spectrum from a suppressed correlation function. In order to ensure that our program would correctly produce this power spectrum, we tested it by inputting the power spectrum predicted by the standard model (and generally confirmed by measurements of the CMB, weak lensing, and large-scale structure, as seen in Figure 5), using a Fourier transform to take this power spectrum to the correlation function, and then using another Fourier transform to take this correlation function back to the power spectrum. If the power spectrum were reproduced correctly, we would know the program was working as it should. These Fourier transforms that formed the basis of the program are shown in Figure 7, below.

$$\xi(r) = \frac{1}{2\pi^2}\int k^2 P(k) j_0(kr) dk = \frac{1}{2\pi^2 r}\int_0^\infty P(k) k sin(kr) dk$$

$$\xi(r)\int_0^\infty r^2 j_0(k'r) dr = \frac{1}{2\pi^2}\int k^2 P(k) dk \int_0^\infty r^2 j_0(kr) j_0(k'r) dr$$

$$\xi(r)\int_0^\infty r^2 j_0(k'r) dr = \frac{1}{2\pi^2}\int k^2 P(k) dk \frac{\pi}{2k^2}\delta(k-k')$$

$$\xi(r)\int_0^\infty r^2 j_0(k'r) dr = \frac{1}{4\pi} P(k')$$

$$P(k') = 4\pi \int_0^\infty r \frac{sin(k'r)}{k'}\xi(r) dr$$

Figure 7: Fourier transform of the power spectrum and correlation function

The program was able to successfully produce the correlation function; Figure 8 shows both the original power spectrum and the resulting correlation function.

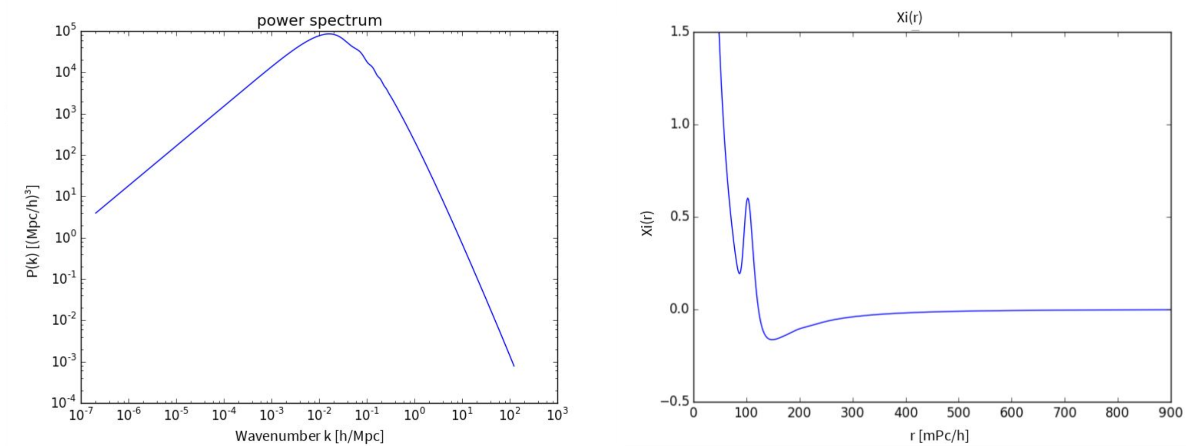

Figure 8: Original power spectrum and resulting correlation function

Once again, note that the graph in Figure 8 looks different from the one in Figure 6 because the correlation function used in Figure 7 and depicted in Figure 8 uses the spatial correlation function rather than the angular correlation function used in Figure 6. Unfortunately, though the program was able to take the Fourier transform of the power spectrum to the correlation function, it was unable to correctly reproduce the original power spectrum. Figure 9 shows its attempt to do so.

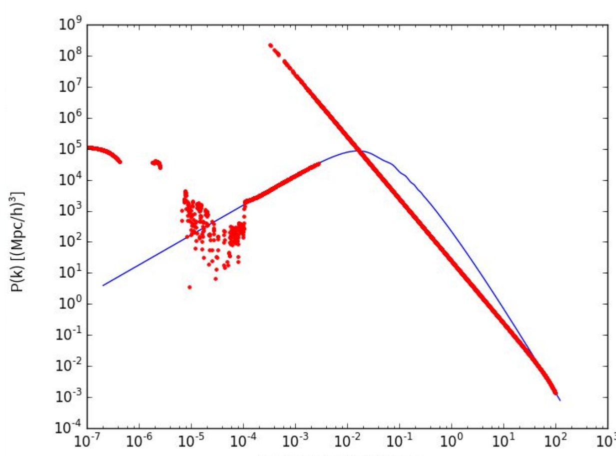

Figure 9: Failed attempt to reproduce the power spectrum

In Figure 9, the blue line represents the original power spectrum and the red dots show the reproduction. Upon inspection of the routine used to integrate the correlation function, we decided to try dividing the integral into several sections. These four sections each have an equal number of points in the correlation function; because the points in the correlation function are on a logarithmic scale, however, this division does not mean that the ranges of each integral are equal. Figure 10 shows each of these integrals. These integrals were then summed to form the recovered power spectrum shown in Figure 11.

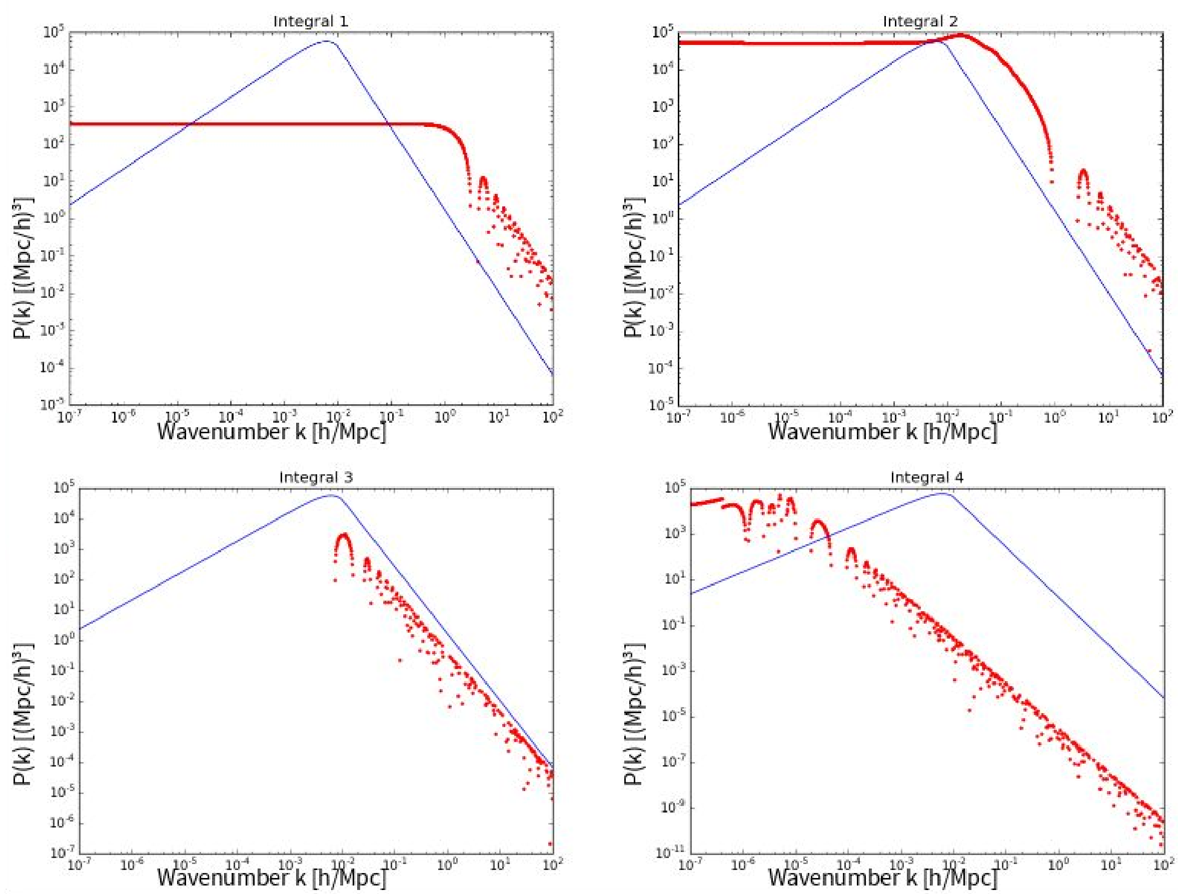

Figure 10: Integrals 1-4

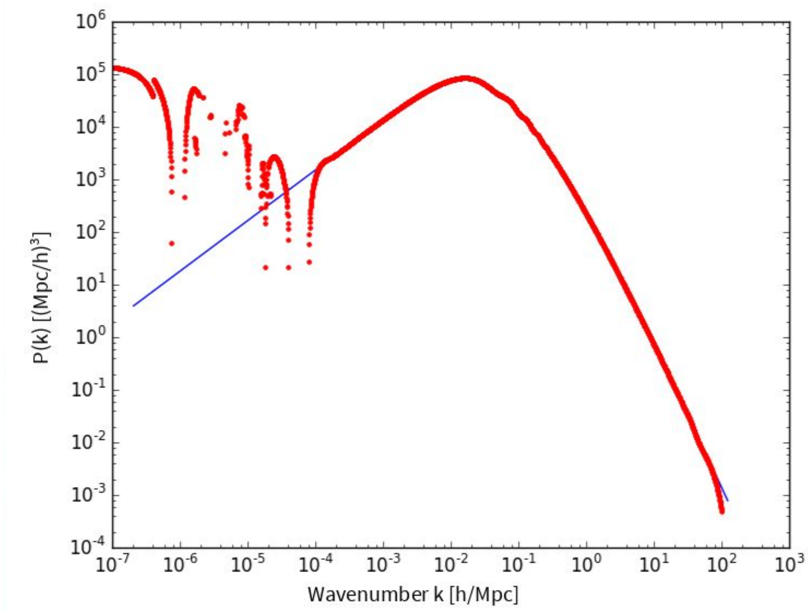

Figure 11: Summation of the four integrals

While this technique produced a noticeably better result, the program was still unable to recreate the low-wavenumber elements of the power spectrum. Unfortunately, due to the form of the integration routine's inputs, this separation of integrals prevented the limits of integration from being completely accurate. Most regrettably, this end of the power spectrum is most important to the project - the high-angular scales where the suppression in the correlation function is seen corresponds to the low wavenumbers where the program fails.

To further test the integration routine, we replaced the LCDM power spectrum with a simple Gaussian function. With this simple Gaussian, Figure 7 yields Equation 1, below, which can be integrated analytically.

$$\int_0^\infty \frac{\exp(-k^2)\, k \sin(k\, r)}{2\, \pi^2\, r}\, dk = \frac{e^{-\frac{r^2}{4}}}{8\, \pi^{3/2}}$$

Referencing Figure 7 shows that the right side of Equation 1 is the correlation function. Again using Figure 7 takes the correlation function back to the power spectrum, shown in Equation 2, below.

$$\int_0^\infty \frac{4\,\pi\, r\,\sin(k\, r)\,\exp\left(-\frac{r^2}{4}\right)}{k\left(8\,\pi^{3/2}\right)}\,dr = e^{-k^2}$$

The corresponding work in our program is shown in Figure 12, below.

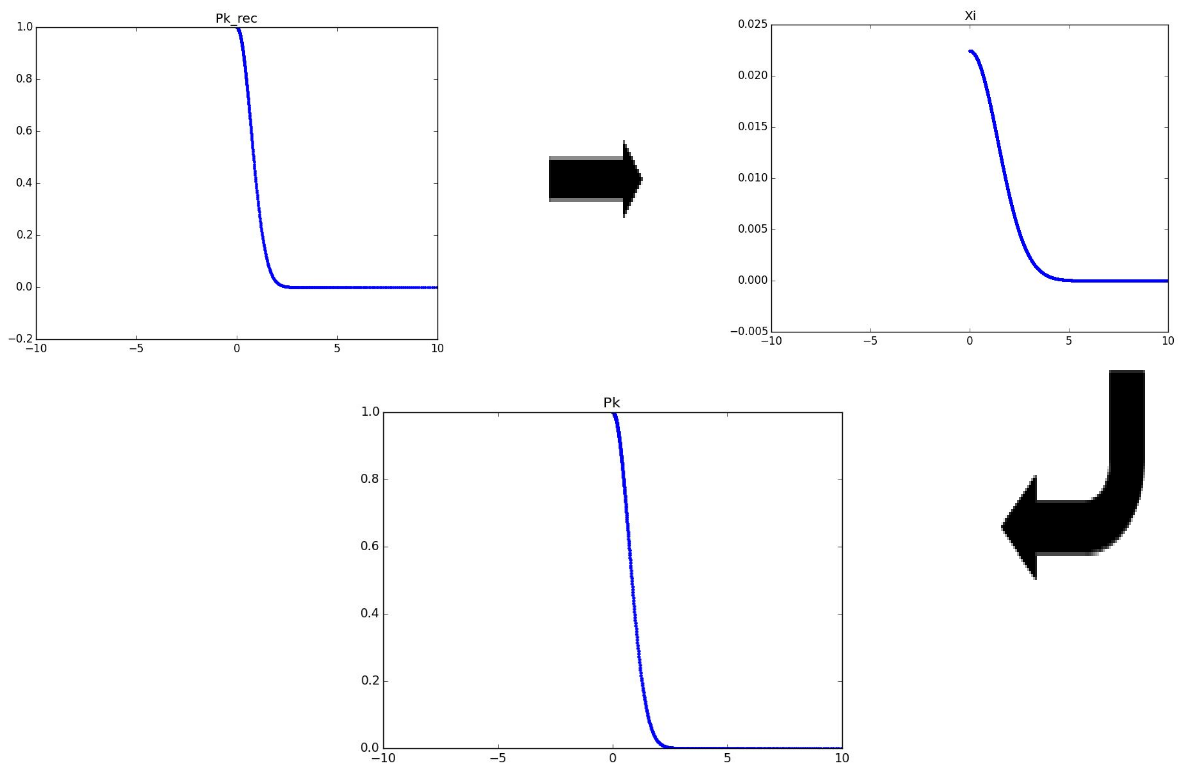

Figure 12: Test of program using a Gaussian

Errors

The fact that the program correctly integrates the Gaussian indicates that the problem is likely specific to the interaction between the power spectrum and the integration routine. The integration routine is numeric, so it divides the area under the graph into sections and approximates each one. It is possible that the miniscule correlation function values at large r-values are too small for the integration routine to compute. While the values of the Gaussian Fourier transform were also small at large r-values, we were able to approximate the Fourier transform of the Gaussian by only integrating to 10 - with the power spectrum, we are forced to integrate to much larger values to approximate the integral to infinity.

Conclusion

As stated above, we were unfortunately not yet able to reproduce the power spectrum through Fourier transforms. Though the initial Fourier transform seems to work, and we are able to produce a correct correlation function, the reproduced power spectrum is incorrect, particularly at small wavenumbers, which is where we would see the result of a suppressed correlation function. Our program was able to successfully Fourier transform a simple Gaussian function and then reproduce the original, which implies that the numeric integration routine is interacting badly with the more complicated, true power spectrum. In the future, we will test the program to see if the division of integrals is necessary - adding more intervals to a single integration should have the same effect. We will also test the integration while watching specific values of the power spectrum. Hopefully, “following” a wavenumber that is incorrectly reproduced will provide insight into the flaws in the program. Finally, we will work to reduce the allowed error in the integration routine to try to more accurately measure and transform the large r-values in the correlation function. Once we are able to reproduce the original power spectrum, we will introduce a suppression into the correlation function, imitating the large-angle suppression observed by COBE and WMAP. From this correlation function, we will generate a power spectrum, which we will feed into CLASS. CLASS will produce large-scale structure and polarization maps, which we can compare to what is observed in our sky. If these maps that were generated with a suppressed power spectrum fit the observed universe better than those generated without a suppressed power spectrum, it would suggest that standard model of cosmology is flawed and needs revision, rather than that we live in a rare “fluke” universe with an unsuppressed power spectrum that happens to produce an odd correlation function.

Thank you to Ted, Arthur, and Dr. Shaun Serej. You’ve given me great opportunities and I would not be here without your guidance.

References

C.L. Bennett et al., "First Year Wilkinson Microwave Anisotropy Probe (WMAP) Observations: Preliminary Maps and Basic Results," Astrophysical Journal Supplement, 148, 1(2003).

C.J. Copi, D. Huterer, D. Schwarz, G.D. Starkman, "No large-angle correlations on the non-Galactic microwave sky," Monthly Notices of the Royal Astronomical Society, 399, 295 (2009).

C.J. Copi, D. Huterer, D. Schwarz, G.D. Starkman, "Large-angle cosmic microwave background suppression and polarization predictions," Monthly Notices of the Royal Astronomical Society, 434, 3590 (2013).

E.F. Bunn and A. Bourdon, “Contamination cannot explain the lack of large-scale power in the cosmic microwave background radiation,” Physical Review D, 78, 123509 (2008).
P.A.R. Ade et al. (Planck collaboration), “Planck 2013 results. I. Overview of products and scientific results,” Astronomy and Astrophysics, 571, A1 (2014).

W. Hu and S. Dodelson, "Cosmic microwave background anisotropies," Annual Reviews
of Astronomy and Astrophysics, 40, 171 (2002).

NASA / WMAP Science Team WMAP # 121238 9 year WMAP image of background cosmic radiation (2012). Retrieved from: https://en.wikipedia.org/wiki/Cosmic_microwave_background#/media/File:Ilc_9yr_moll4096.png

National Science Foundation (NASA, JPL, Keck Foundation, Moore Foundation, related) - Funded BICEP2 Program (2014). Retrieved from: https://en.wikipedia.org/wiki/Chronology_of_the_universe#/media/File:History_of_the_Universe.svg

Jaffe, A. H., & Gaweiser, E. (1999). WOMBAT & FORECAST: Making Realistic Maps of the Microwave Sky. Retrieved from: https://ned.ipac.caltech.edu/level5/Sept05/Gawiser2/Gawiser3.html

ESA (European Space Agency), (2013). Retrieved from: http://sci.esa.int/planck/51563-all-sky-maps-of-the-cosmic-microwave-background-at-nine-frequencies/

Tegmark, M. et al. 2004. PhRvD, 69, (10), 103501. Retrieved from: https://ned.ipac.caltech.edu/level5/Sept11/Norman/Norman_refs.html#tegmark03

Chiacchia, K. (2012). Bright Lights, Big Cosmos. *Projects in Scientific Computing*. Retrieved from: http://psc.edu/science/2012/cosmos/

Sarkar, D., Huterer, D., Copi, C. J., Starkman, G. D., & Schwarz, D. J. (2011). Missing power vs low-ℓ alignments in the cosmic microwave background: No correlation in the standard cosmological model. *Astroparticle Physics, 34*(8), 591-594.